Microsyst Technol (2017) 23:1207–1214
DOI 10.1007/s00542-015-2804-0

TECHNICAL PAPER

Label-free detection of prostate specific antigen (PSA) using a bridge-shaped PZT resonator

Dong Gun Hwang[1] · Youn Mee Chae[1] · Nakwon Choi[1] · Il-Joo Cho[1] · Ji Yoon Kang[1] · Soo Hyun Lee[1]

Received: 5 November 2015 / Accepted: 29 December 2015 / Published online: 5 January 2016

Abstract This paper reports the results of the development and testing of a bridge-shaped resonator to detect different concentrations of prostate specific antigen (PSA) based on shifts in resonant frequency. The bridge-shaped PZT resonator was fabricated by Micro Electro Mechanical Systems techniques, including photolithography, wet and dry etching, and film deposition. The prototype consists of multiple layers comprised of Ta/Pt/PZT/Pt followed by a supporting layer of SiN_x. The resonant frequency of the bridge-shaped PZT resonator was measured in the air by a heterodyne laser doppler vibrometer, and the frequencies were 406 ± 3, 177 ± 2, and 121 ± 1 kHz for the dimensions of 50 μm × 250 μm, 100 μm × 500 μm, and 150 μm × 750 μm (width × length), respectively. Bridge-shaped PZT resonators of different geometries have been used to detect PSA over a wide range of concentrations from 10 pg/ml to 100 ng/ml, which includes the clinically relevant diagnostic range. Using the specific binding between PSA and PSA antibody, different concentrations of PSA can be detected through the change of resonant frequency caused by the mass of the bound PSA. The measured resonant frequency and the calculated mass of bound PSA were used to calculate mass sensitivity ($S = \Delta f/\Delta m$). Mass sensitivities of bridges with dimensions of 50 μm × 250 μm, 100 μm × 500, and 150 μm × 750 μm were 44.14, 18.90 and 8.31 Hz/pg, respectively. This shows that mass sensitivity increases as the dimensions of the bridge get smaller. The feasibility of detecting 10 pg/ml of PSA was confirmed, which is a much smaller amount than 4 ng/ml, which is the conventional cut-off point between a patient and a non-patient in clinical diagnostics.

1 Introduction

Recently, research on biosensors using Micro Electro Mechanical Systems (MEMS) and Nano Electro Mechanical Systems (NEMS) has progressed actively (Benecke 1989; Flynn et al. 1992; Polla 1997). Generally, the methods used in biosensors to detect proteins, DNA, and RNA are classified as label-based or label-free detection methods (Ray et al. 2010). Common examples of the label-based detection method include fluorescent, chemiluminescent, and radioactive labeling. These label-based detection methods have synthetic challenges and multiple label issues, and they may exhibit interference with the biding sites (Yu et al. 2006). Therefore, the development of sensitive, reliable, high-throughput, label-free detection techniques is now attracting significant attention. Typical examples of label-free detection methods are surface plasmon resonance (SPR) (Wassaf et al. 2006), ellipsometry-based techniques (Chamritski et al. 2007), interference-based techniques (Ozkumur et al. 2008), and micro resonators (Lerman and Elata 2010). Currently, a micro resonator that utilizes advanced MEMS and NEMS techniques is receiving a significant amount of attention from engineers in the field.

In general, micro resonators are classified into three categories depending on shape, i.e., diaphragm, cantilever, and bridge (Chengkuo et al. 1996; Polla 1997). The quartz-crystal micro-balance (QCM), which is used widely as a biosensor, is one of the diaphragm-shaped resonators. The advantages of the QCM include good frequency stability and reproducibility for detecting target materials. However, the QCM is not easy to use as a sensor when it

✉ Soo Hyun Lee
dream.ideal@gmail.com; shleekist@kist.re.kr

[1] Center for BioMicrosystems, Korea Institute of Science and Technology, Seoul 136-791, Republic of Korea

must be integrated with other components. In addition, it is not compatible with the process for MEMS fabrication or conventional semiconductor fabrication because of its own material properties, and it has a low sensitivity to changes in mass due to its relatively low operating frequency (Xu et al. 2008).

Cantilever-shaped resonators are the most well-known of the micro resonators. They have been produced at the nano scale and investigated intensely (Ilic et al. 2005). The silicon-based cantilever resonator especially has been actively researched due to its availability and its easy integration with silicon-based technology. However, silicon-based cantilever resonators require an expensive optical apparatus because they cannot acquire a direct electrical signal (Lee et al. 2005). Also, in general, they have optical limitations, such as a narrow dynamic range and parasitic deflection in optical measurements. Also, silicon-based cantilever resonators are measurable in very high vacuum state (Ilic et al. 2001). To overcome these disadvantages, micro resonators using PZT (a piezoelectric material) currently are being investigated. A resonator using PZT is capable of electrically driving and sensing mechanical resonance due to its piezoelectric characteristic (Lee et al. 2005). Also, the high actuating characteristics of PZT make detection possible at room temperature and atmospheric pressure. However, the shape of cantilever resonators is problematic. One side of the cantilever has a fixed end, while the other side has a free-standing end. When small particles, including proteins and DNA, are deposited on the cantilever, they alter the effective mass, causing a shift in the resonant frequency (Forsen et al. 2005; Rogers et al. 2003). In addition, the tendency of the target materials to adhere to the cantilever resonator induces changes in the surface stress and also shifts the resonant frequency (Tzou et al. 2004). Whether one of these changes dominates the shift in the resonant frequency is still a matter of debate. To overcome the shortcomings of the cantilever resonator, a bridge-shaped resonator clamped on both sides has been the subject of recent research efforts. Bridge-shaped resonators have excellent mass sensitivity compared to other biosensors with different shapes (Shin et al. 2005; Zang et al. 2001).

Prostate specific antigen (PSA) is the most reliable clinical marker for detecting prostate cancer and for monitoring the progression of the disease (Lee et al. 2005; Wu et al. 2001). Prostate cancer is the most prevalent form of cancer in men, and it ranks second in the number of cancer deaths it causes among men in the United States (Hwang et al. 2004). The Center for Disease Control (CDC) reported that 223,307 men were diagnosed with prostate cancer in 2007 and that 29,093 men died from this cancer in 2007, the latest year for which such statistics were available. Prostate cancer causes PSA to be released into the circulatory system, and the PSA level in the blood can be increased by a factor of 10^5. The minimum threshold for detecting prostate cancer is 4 ng/mL (Lilja et al. 2008). Generally, PSA is detected using ELISAs. However, ELISA analysis requires multiple steps and also requires a label for detection of the analyte (Wu et al. 2001).

In this paper, we describe bridge-shaped resonators using PZT that were fabricated to verify the feasibility of their use as biosensors. Using a heterodyne laser doppler vibrometer (LDV), the resonant frequency of the bridge-shaped resonator was measured in the air environment. In contrast to ELISA, the bridge-shaped PZT biosensors require no label and can function using a single reaction without additional reagents. Based on specific binding between PSA and PSA antibody, different concentrations of PSA were detected through the change of resonant frequency caused by the mass of PSA bound with PSA antibody. The resonant frequencies that were measured and the mass of PSA bound with antibody that was calculated were used to calculate mass sensitivity.

2 Materials and methods

2.1 Fabrication of bridge-shaped PZT resonators

By low pressure chemical vapor deposition (LPCVD), a low-stress silicon nitride (SiN_x) thin film (1 μm) was deposited on a 4-inch silicon wafer. Then, as a bottom electrode, a Ta adhesive layer with a thickness of 30 nm was deposited by DC magnetron sputtering, followed by the deposition of a Pt layer with a thickness of 150 nm. The PZT film, which was manufactured by the diol-based, sol–gel method, was spin-coated to a thickness of 1 μm by 12 replications of the spin-coating method. Sputtering was used to deposit Pt at a thickness of 100 nm to serve as the top electrode layer. Photolithography was required as a preprocessing technique, using AZ 7220 photoresistor (AZ Electronic Materials, USA) to etch the designated area of the bridge. The top Pt layer, PZT, and bottom Pt layer were etched by an advanced oxide etcher (AOE) successively in order to shape the bridge. Also, part of the bottom Pt layer was used as an electrical pad. By plasma enhanced chemical vapor deposition (PECVD), SiO_2 layer was deposited to a thickness of 300 nm; then, it was etched partially using reactive ion etching (RIE) for making both the insulator layer and the buffer layer to compensate for the height difference between the top and bottom layers of Pt. The lift-off method was used to deposit Ti/Pt (30/300 nm) on a specific area of SiO_2 layer. This process connected the electrical pad with the top Pt layer. For releasing the bridge, SiN_x layer on the back of the wafer was etched by RIE, leaving a patterned area with a photoresistor. Then, the bulk silicon was wet etched with a 30 %

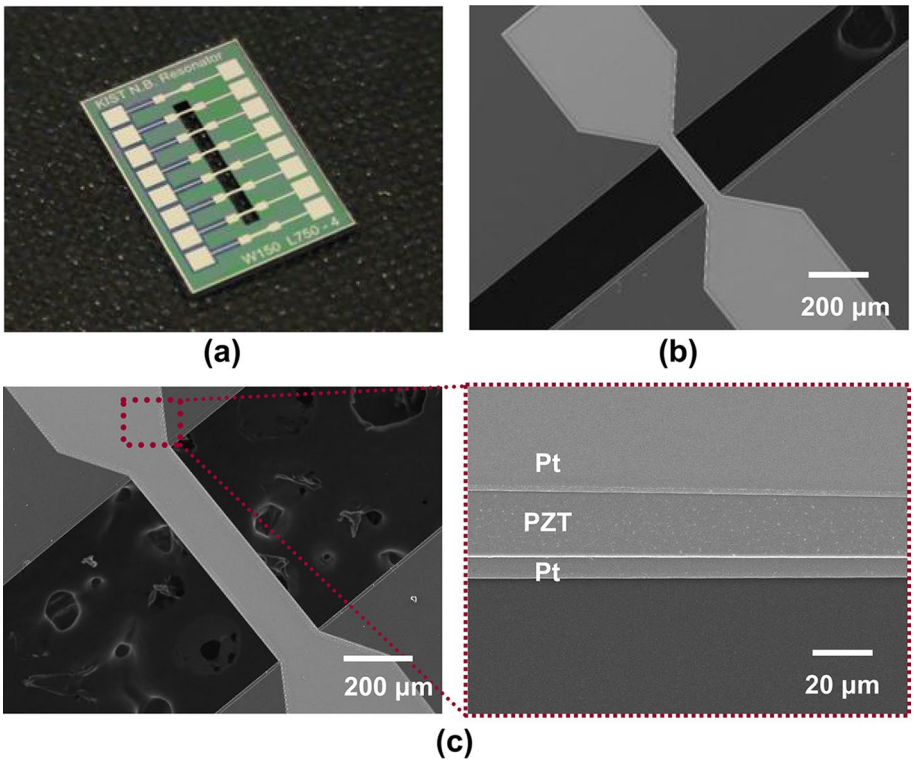

Fig. 1 Photograph and SEM images of bridge-shaped PZT resonators: **a** one device including six active resonators, **b** 50 μm × 250 μm dimension of resonator, and **c** 150 μm × 750 μm dimension of resonator

KOH silicon etchant. Finally, SiN_x was removed by RIE, completing the fabrication procedure for the bridge-shaped resonator. In one completed wafer, there are 52 devices with the dimensions of 8 mm × 12 mm, and each device has six active resonators and two reference resonators. In such devices, there are three different kinds of bridge arrays with dimensions (w × l) of 50 μm × 250 μm, 100 μm × 500 μm, and 150 μm × 750 μm. The arrays were separated by using a femtosecond laser micromachining workstation (MicroablaterTM M-2000, Exitech, Oerlikon Optics, Ltd., UK) to form a single device. In Fig. 1, photograph and SEM images show the bridge-shaped PZT resonators: (a) one device including six active resonators, (b) 50 μm × 250 μm dimension of resonator, and (c) 150 μm × 750 μm dimension of resonator.

2.2 Bioassay

2.2.1 Formation of self-assembly monolayer (SAM)

An antibody of PSA must be immobilized on the surface of the bridge in order to conduct a quantitative analysis of PSA using the antibody-antigen specific interaction. To attach the antibody on the surface of the bridge, there must be a self-assembly monolayer (SAM) to serve as a linker between the surface of the bridge and the antibody. In this research, calixcrown (Calixarene derivative) SAM was used as the linker to fix the antibody on the surface of the gold. Because the SAM has a special ability to recognize the ammonium ions of proteins, protein is immobilized on its surface (Lee et al. 2005). In order to build the calixcrown SAM, an e-beam evaporator must be used to deposit Cr and Au layers on the SiN_x (backside of the bridge) with thicknesses of 10 and 50 nm, respectively. Organic materials and other contaminants are removed by cleaning with piranha solution [a ratio of H_2O_2 (34 %) to H_2SO_4 (98 %) of 1:3] and de-ionized water. Next, the resonator is placed in a 3 mM calixcrown solution mixed with chloroform (CH_3Cl) solvent. Finally, the calixcrown SAM is formed on the gold surface as a result of chemical adsorption between thiol of calixcrown-end and Au surface.

2.2.2 Immobilization of PSA antibody and antigen

The resonator with the calixcrown SAM is placed in a solution of the phosphate buffered saline (PBS) diluted with a specific monoclonal anti-prostate antibody at a concentration of 10 μg/ml for an hour. During this process, the calixcrown SAM and PSA antibody combine and become fixated on the surface of the bridge. After the fixation process, unfixed-protein on the surface is washed with PBS buffer (pH 7.4) mixed with polyoxyethylene sorbitan monolaurate (Tween 20, St. Louis, MO, USA) and desiccated with nitrogen gas. Next, to prevent non-specific binding, the resonator is put into the PBS buffer mixed with 1 mg/ml of bovine serum albumin (BSA) (Sigma, St. Louis, MO, USA) for an

hour. This procedure prevents PSA from binding with the SAM on the gold in a random fashion, thereby preventing changes in the resonant frequency due to non-specific binding. The unabsorbed residual BSA is cleansed with PBS buffer (pH 7.4) mixed with polyoxyethylene sorbitan monolaurate and then it is cleansed with PBS buffer again.

For antibody-antigen interaction, PSA antibody that is immobilized on the bridge-shaped resonator is soaked in PSA solutions with various concentrations for an hour. And then, it is cleansed with PBST (PBS with Tween 20, St. Louis, MO, USA) and then PBS buffer again. It is desiccated with nitrogen gas.

In order to verify specific binding between PSA and PSA antibody using a laser confocal scanner, PSA is labeled with a fluorescent material, Cy3 (Amersham Biosciences, Piscataway, NJ, USA). To evaluate the performance of the bridge-shaped resonator as a biosensor, the change of the resonant frequency caused by specific binding is measured while the concentration of PSA was changed from 100 pg/ml to 100 ng/ml in 10 increments using resonators with three different dimensions (w × l), i.e., 50 μm × 250 μm, 100 μm × 500 μm, and 150 μm × 750 μm.

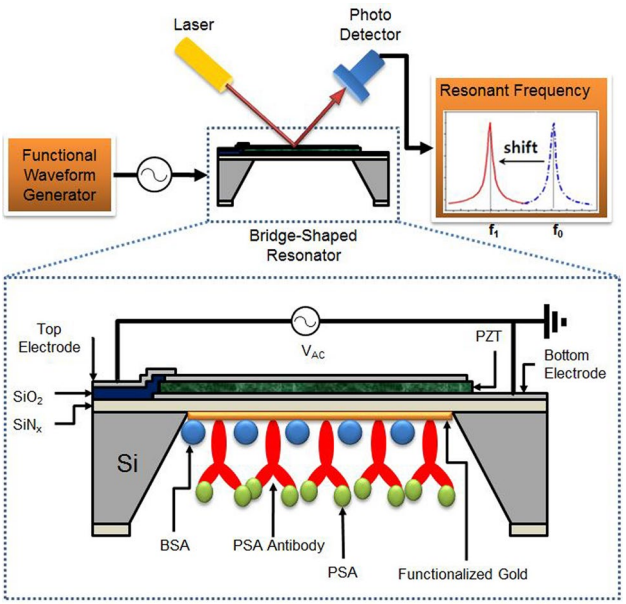

Fig. 2 Experimental setup for bridge-shaped PZT resonator and sensing system for detecting PSA

2.3 Measurement of resonant frequency

The resonant frequency of the bridge-shaped resonator is measured using an optical heterodyne laser doppler vibrometer (LDV) (MLD211D, Neo Ark Co., Japan) in an air environment. The experimental setup is shown in Fig. 2. A function waveform generator (33120A, Agilent) is used for generating a sinusoidal waveform voltage, which is applied to the actuation (top) electrode while the bottom electrode is grounded. The vibration of the bridge-shaped resonator is determined by the vibrometer to be a sweeping frequency with a sinusoidal waveform in the designated range of frequency, and the resonant frequency was measured in such a way as to determine the highest value of vibration velocity. Through the procedure above, changes in resonant frequency were measured in each immunoassay step, such as the depositions of Cr/Au, SAM, antibody, BSA and antigen. Our experiments were focused specifically on measuring the changes in resonant frequency that occurred with different concentrations of PSA.

3 Results and discussion

3.1 Theoretical analysis

Every material has its own frequency, called its natural frequency, and some materials have several natural frequencies. When physical forces act on an object at the same frequency as the natural frequency of the target object, the displacement caused by vibration increases considerably. This phenomenon is called resonance, and the frequency at which it occurs is called the resonant frequency.

Resonant frequency has its own specific value depending on structures. A mechanical structure that uses this characteristic is called a resonator, and resonant frequency varies with mechanical characteristics, such as the shapes and properties of materials that act as resonators. The resonant frequency of an oscillating bridge-shaped resonator can be expressed as:

$$\mathrm{f} = \frac{1}{2\pi}\sqrt{\frac{k}{m}} \tag{1}$$

where k is the spring constant, and m is the effective mass of the resonator. From Eq. 1, the theoretical frequency change based on mass change can be derived as shown below. The term f_0 is the resonant frequency before mass loading, and f_1 is the resonant frequency after mass loading, as shown in Eqs. 2 and 3.

$$f_0 = \frac{1}{2\pi}\sqrt{\frac{k}{m}} \tag{2}$$

$$f_1 = \frac{1}{2\pi}\sqrt{\frac{k}{m+\Delta m}} \tag{3}$$

These two equations can be combined into one equation that represents mass change (Δm), as shown below:

$$\Delta \mathrm{m} = \frac{k}{4\pi^2}\left(\frac{1}{f_1^2} - \frac{1}{f_0^2}\right) \tag{4}$$

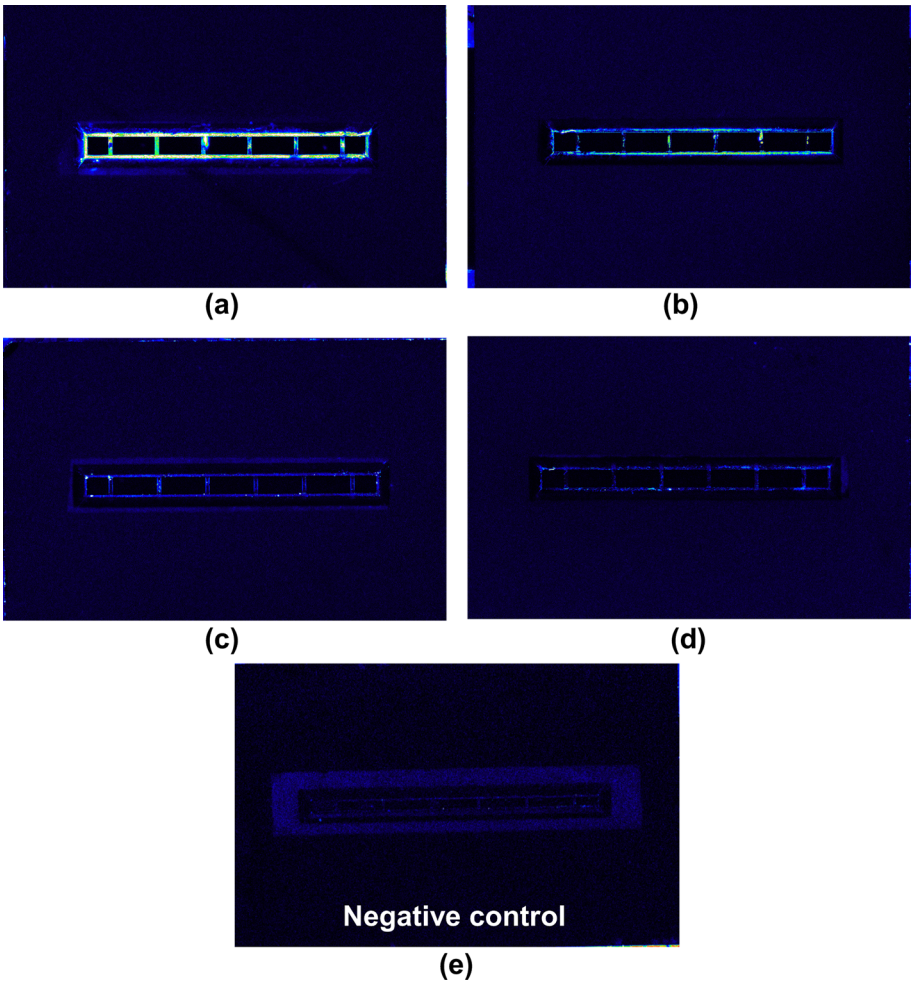

Fig. 3 Fluorescent scanner images based on PSA labeled with Cy3 concentrations of **a** 100 ng/ml, **b** 10 ng/ml, **c** 1 ng/ml, **d** 100 pg/ml, and **e** 1 mg/ml of HSA as a negative control

From Eq. 4, the mass changes of a bridge-shaped resonator directly reflect changes in the resonant frequency. Thus, changes in the mass of the resonator can be determined based on observed changes of the resonant frequency. Accordingly, a bridge-shaped resonator has high potential for use as a biosensor because it can detect specific biomolecules, such as DNA, antibody, and antigen, based on changes in their masses.

Mass sensitivity (S) is defined as the change in resonant frequency corresponding to a unit mass loading. Thus, higher sensitivity implies that very small changes in mass cause considerable changes in the resonant frequency. This relationship is shown in Eq. 5.

$$\mathrm{S} = \frac{\Delta f}{\Delta m} \tag{5}$$

Here, Δf is the amount of change in the resonant frequency caused by a change in the mass, and Δm is the change in the mass. The units of S are Hz/g. The larger the absolute value of S becomes, the more sensitive the resonator is. Given the assumption that the spring constant remains constant during mass loading, Eq. 4 can be simplified into Eq. 6 by combining $f_1 = f_0 - \Delta f$ and $\Delta f \ll f_0$.

$$\Delta \mathrm{m} \propto \frac{\Delta f}{f_0^3} \tag{6}$$

Therefore, high mass sensitivity can be achieved because the higher the resonant frequency of a resonator is, the smaller the mass change it can detect. Among three different dimensions of bridge-shaped resonators, the dimension of 50 μm × 250 μm has the highest mass sensitivity because of the highest resonant frequency.

3.2 Quantitative PSA analysis using fluorescent image

To confirm specific binding between PSA and PSA antibody optically, PSA labeled with Cy3 with concentrations of 100, 10, 1 ng/ml, and 100 pg/ml were immunoassayed using the bridge-shaped resonators on which PSA antibody was immobilized. Then, fluorescent scanner images were observed with a laser confocal scanner (GSI Group Inc., USA), as shown in Fig. 3. As a result, specific binding between PSA and PSA antibody only occurs when the PSA antibody is immobilized on the surface of the Au by a monomolecular layer of calixcrown SAM. We can see

distinctive changes in the confocal intensity based on different concentrations of PSA. Quantitative results indicated that the intensity of the fluorescence increased as the concentration of PSA increased.

Also, to verify a degree of non-specific binding between the PSA antibody and the heterogeneous protein, 1 mg/ml of human serum albumin (HSA) labeled with Cy3 instead of PSA was immunoassayed to serve as a negative control. As shown in Fig. 3e, the fluorescent image indicated that there was negligible non-specific binding between the PSA antibody and the HSA protein, which means that the PSA antibody has high specificity for PSA. Overall, specific binding between PSA and PSA antibody occurs only on the bridge on which Au has been deposited, and quantitative binding occurs according to the concentration of PSA. Non-specific binding between PSA antibody and HSA protein is negligible. These results ensure that the bridge-shaped resonator with immobilized PSA antibody can detect PSA among various kinds of proteins in body fluid.

3.3 Characterization of resonant frequency shift (based on mass change)

Using heterodyne laser doppler vibrometer (LDV), the resonant frequencies of the bridge-shaped resonators were measured in an air environment before immunoassay. The resonant frequencies were determined to be 406 ± 3, 177 ± 2, and 121 ± 1 kHz for dimensions of 50 μm × 250 μm, 100 μm × 500 μm, and 150 μm × 750 μm (width × length), respectively.

Bridge-shaped resonators with dimensions of 50 μm × 250 μm and 100 μm × 500 μm were used for immunoassay with 100 ng/ml of PSA. The resonant frequency shifts shown in Fig. 4 are based on the order of Cr/Au deposition, calixcrown SAM formation, PSA antibody adsorption, BSA treatment, and PSA adsorption. By comparing Fig. 4a, b, we were able to determine that the graphs of resonant frequency changes had the same pattern with different quantities.

Next, the resonant frequency changes were measured using 0.01, 0.1, 1.0, 10, and 100 ng/ml of PSA, as shown in Fig. 5a. In the case of the bridge-shaped resonators with dimensions of 50 μm × 250 μm, 100 μm × 500 μm, and 150 μm × 750 μm, specific binding occurred between PSA and PSA antibody, which caused the resonant frequency to decrease. Moreover, as the concentration of PSA decreased, the amount of change in the resonant frequency also decreased. The bridge-shaped resonator with a dimension of 150 μm × 750 μm had resonant frequency decreases of 93.90, 57.05, 31.30, 7.83, and 6.26 Hz for PSA concentrations of 100, 10, 1 ng/ml, 100, and 10 pg/ml, respectively. Likewise, the bridge-shaped resonator with a dimension of 100 μm × 500 μm had resonant frequency

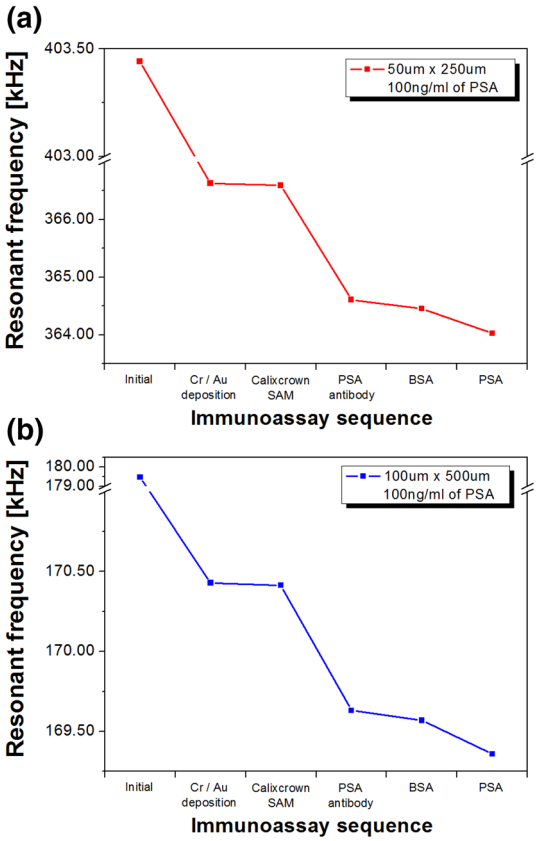

Fig. 4 Resonant frequency shift during immunoassay, which includes Cr/Au deposition, calixcrown SAM formation, PSA antibody adsorption, BSA treatment, and PSA adsorption on the bridge-shaped resonator with dimensions of **a** 50 μm × 250 μm and **b** 100 μm × 500 μm

decreases of 210.06, 114.11, 67.43, 23.34, and 9.40 Hz for the PSA concentrations listed above, respectively. In addition, the bridge-shaped resonator with a dimension of 50 μm × 250 μm had resonant frequency decreases of 427.80, 292.87, 197.37, 65.00, and 22.90 Hz for the same PSA concentrations, respectively. Each reported decrease of a resonant frequency value is an average of the results obtained for 30 experiments that were repeated at the same conditions.

To compare bridge-shaped resonators with three different dimensions, the resonant frequency decreases caused by 1 ng/ml of PSA were 31.30, 67.43, and 197.37 Hz for dimensions of 150 μm × 750 μm, 100 μm × 500 μm, and 50 μm × 250 μm, respectively, from which it can be concluded that, at the same concentration of PSA, the changes in the resonant frequencies increased as the dimensions decreased. Therefore, we know that the mass sensitivity increases as the dimensions of the bridge-shaped resonator decrease.

As mentioned in 3.1, using correlation analysis between mass change (Δm) and resonant frequency change (Δf)

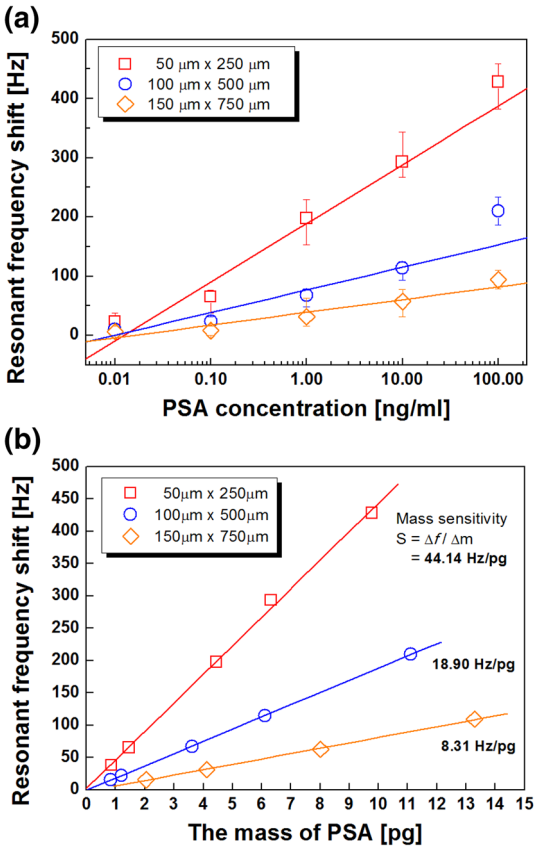

Fig. 5 Resonant frequency shift as a function of **a** PSA concentration and **b** the mass of PSA absorbed with PSA antibody for different dimensions of bridge-shaped resonators

makes it possible to analyze PSA quantitatively. From Eq. 4, the quantitative analysis was performed based on the results of detecting different concentrations of PSA for each bridge-shaped resonator, as shown in Fig. 5b. In the bridge-shaped resonator with dimensions of 50 μm × 250 μm, we calculated the mass of PSA absorbed with PSA antibody based on the resonant frequency changes. The mass of PSA was 9.79, 6.32, 4.46, 1.46, and 0.86 pg for PSA concentrations of 100, 10, 1, 100, and 10 pg/ml, respectively. Similarly, in the bridge-shaped resonator with dimensions of 100 μm × 500 μm, the mass of PSA absorbed with PSA antibody was 11.12, 6.13, 3.62, 1.20, and 0.83 pg for the same PSA concentrations; the bridge-shaped resonator with dimensions of 150 μm × 750 μm had 13.29, 8.02, 4.12, 2.04, and 1.05 pg. Using the above results, the mass sensitivities (S = Δf/Δm) of the bridge-shaped resonators with dimensions of 50 μm × 250 μm, 100 μm × 500 μm, and 150 μm × 750 μm were calculated to be 44.14, 18.90, and 8.31 Hz/pg, respectively. Also, to verify changes of resonant frequency caused by non-specific binding between heterogeneous protein and PSA antibody, HSA with a concentration of 1 mg/ml was immunoassayed with PSA antibody immobilized on the three different designs of the resonator. The results of resonant frequency changes caused by different concentrations of PSA and HSA are shown in Table 1. Considering the resonant frequency changes caused by PSA and HSA, PSA can be detected in the 10 pg/ml range using the bridge-shaped resonator with dimensions of 50 μm × 250 μm, whereas PSA in the and 100 pg/ml range can be detected by the bridge-shaped resonator with dimensions of 100 μm × 500 μm. In addition, the bridge-shaped resonator with dimensions of 150 μm × 750 μm was able to detect PSA in the 1 ng/ml range. Thus, the feasibility of detecting 10 pg/ml of PSA was confirmed using the bridge-shaped resonator with dimensions of 50 μm × 250 μm, which is much less than a PSA concentration of 4 ng/ml, which is currently the cut-off point between a patient and a non-patient in clinical diagnostics.

4 Conclusions

In this research, bridge-shaped PZT resonators based on MEMS technologies were fabricated and applied as biosensors to evaluate their ability to detect PSA through specific binding between PSA and PSA antibody, which causes resonant frequency changes. To detect and analyze PSA quantitatively using the fabricated bridge-shaped resonators, various procedures were performed in order to conduct the PSA assay, including the deposition of Au on the backside of the bridge, the formation of calixcrown SAM, and the immobilization of PSA antibody. By using resonators with dimensions of 50 μm × 250 μm, 100 μm × 500 μm, and 150 μm × 750 μm, the results of detecting PSA showed that the resonant frequency decreases because the mass changes by specific binding between PSA and PSA antibody. Also, as PSA concentration decreased to 100, 10, 1 ng/ml, 100, and 10 pg/ml, the amount of change in the resonant frequency decreased. That is, specific binding

Table 1 Comparison of measured resonant frequency shift with respect to each concentration of PSA and 1 mg/ml of HSA

Dimension	HSA	PSA				
(W × L)	1 mg/ml	10 pg/ml	100 pg/ml	1 ng/ml	10 ng/ml	100 ng/ml
50 μm × 250 μm	16.51 Hz	22.9 Hz	65.00 Hz	197.37 Hz	292.87 Hz	427.80 Hz
100 μm × 500 μm	8.38 Hz	9.40 Hz	23.34 Hz	67.43 Hz	114.11 Hz	210.06 Hz
150 μm × 750 μm	6.71 Hz	6.26 Hz	7.83 Hz	31.30 Hz	57.05 Hz	93.90 Hz

between PSA and PSA antibody caused changes in the mass of the bridge-shaped resonator. To be confident of the reliability of resonant frequency change, fluorescent images were observed in order to confirm specific binding using different concentrations of PSA labeled with Cy3 by means of a laser confocal scanner. It was confirmed that PSA can be bound quantitatively, depending on the concentration of PSA. Comparing bridge-shaped resonators with three different dimensions to detect 1 ng/ml of PSA, the resonant frequency changes increased when the dimensions decreased, indicating that resonators with smaller dimensions have higher mass sensitivity. To apply bridge-shaped resonators as a biosensor for the detection of PSA, it must be verified that they can detect less than 4 ng/ml of PSA, which is the current cut-off point between patient and non-patient. In the case of the bridge-shaped resonators with dimensions of 50 μm × 250 μm, it was possible to detect PSA at the 10 pg/ml level. In addition, through quantitative analysis based on changes in resonant frequencies, we confirmed that the quantity of PSA detected was in the picogram range.

This research proved that bridge-shaped resonators can be applied as highly sensitive biosensors. In the future, we will test the sensitivity of developed bridge-shaped resonators using whole blood or serum containing PSA from patients. And also, we plan to build a new sensing system that will enable us to make electrical measurements in order to detect various proteins in liquid status and in real-time after integrating microfluidic components.

Acknowledgments This research was partially supported by National Research Foundation grant funded by the Korea government (MEST) (Grant No: 2009-0091918, 2010-0020714). And also, this work was partially supported by the KIST Institutional Program (2E25474).

References

Benecke W (1989) Micromechanical sensors. In: CompEuro '89., 'VLSI and Computer Peripherals. VLSI and Microelectronic Applications in Intelligent Peripherals and their Interconnection Networks', Proceedings. pp 3/39–3/47

Chamritski I, Clarkson M, Franklin J, Li SW (2007) Real-time detection of antigen-antibody reactions by imaging ellipsometry. Aust J Chem 60:667–671

Chengkuo L, Itoh T, Suga T (1996) Micromachined piezoelectric force sensors based on PZT thin films Ultrasonics. IEEE Trans Ferroelectr Freq Control 43:553–559

Flynn AM, Tavrow LS, Bart SF, Brooks RA, Ehrlich DJ, Udayakumar KR, Cross LE (1992) Piezoelectric micromotors for microrobots. J Microelectromech Syst 1:44–51

Forsen E et al (2005) Ultrasensitive mass sensor fully integrated with complementary metal-oxide-semiconductor circuitry. Appl Phys Lett 87:043507. doi:10.1063/1.1999838

Hwang KS, Lee JH, Park J, Yoon DS, Park JH, Kim TS (2004) In-situ quantitative analysis of a prostate-specific antigen (PSA) using a nanomechanical PZT cantilever. Lab Chip 4:547–552

Ilic B, Czaplewski D, Zalalutdinov M, Craighead HG, Neuzil P, Campagnolo C, Batt C (2001) Single cell detection with micromechanical oscillators Journal of Vacuum Science and Technology B: microelectronics and nanometer structures 19:2825–2828

Ilic B, Yang Y, Aubin K, Reichenbach R, Krylov S, Craighead HG (2005) Enumeration of DNA Molecules Bound to a nanomechanical oscillator. Nano Lett 5:925–929. doi:10.1021/nl050456k

Lee JH, Hwang KS, Park J, Yoon KH, Yoon DS, Kim TS (2005) Immunoassay of prostate-specific antigen (PSA) using resonant frequency shift of piezoelectric nanomechanical microcantilever. Biosens Bioelectron 20:2157–2162. doi:10.1016/j.bios.2004.09.024

Lerman M, Elata D (2010) On the quality-factor of micro-resonators. Procedia Eng 5:95–98. doi:10.1016/j.proeng.2010.09.056

Lilja H, Ulmert D, Vickers AJ (2008) Prostate-specific antigen and prostate cancer: prediction, detection and monitoring. Nat Rev Cancer 8:268–278

Ozkumur E et al (2008) Label-free and dynamic detection of biomolecular interactions for high-throughput microarray applications. Proc Natl Acad Sci USA 105:7988–7992. doi:10.1073/pnas.0711421105

Polla DL (1997) Application of PZT thin films in microelectromechanical systems Proc. SPIE 3046, Smart Structures and Materials 1997: Smart Electronics and MEMS, 24; doi:10.1117/12.276603

Ray S, Mehta G, Srivastava S (2010) Label-free detection techniques for protein microarrays: prospects, merits and challenges. Proteomics 10:731–748. doi:10.1002/pmic.200900458

Rogers B et al (2003) Mercury vapor detection with a self-sensing, resonating piezoelectric cantilever. Rev Sci Instrum 74:4899. doi:10.1063/1.1614876

Shin S, Lee N, Park H, Park J, Lee J (2005) Piezoelectrically driven microtransducer mass sensors integrated ferroelectrics 76:93–100. doi:10.1080/10584580500413723

Tzou H, Lee HJ, Arnold S (2004) Smart Materials. Precision sensors/actuators, smart structures, and structronic systems mechanics of advanced materials and structures 11:367–393. doi:10.1080/15376490490451552

Wassaf D et al (2006) High-throughput affinity ranking of antibodies using surface plasmon resonance microarrays. Anal Biochem 351:241–253. doi:10.1016/j.ab.2006.01.043

Wu G, Datar RH, Hansen KM, Thundat T, Cote RJ, Majumdar A (2001) Bioassay of prostate-specific antigen (PSA) using microcantilevers Nat. Biotech 19:856–860

Xu T, Wang Z, Miao J, Yu L, Li CM (2008) Micro-machined piezoelectric membrane-based immunosensor array. Biosens Bioelectron 24:638–643. doi:10.1016/j.bios.2008.06.024

Yu X, Xu D, Cheng Q (2006) Label-free detection methods for protein microarrays proteomics 6:5493–5503. doi:10.1002/pmic.200600216

Zang M, Zurn SM, Robbins WP, Polla DL, Markus D (2001) Bridge structure PZT thin film microtransducer with mass loading", Proc. SPIE 4435, Wave Optics and VLSI Photonic Devices for Information Processing, 152; doi:10.1117/12.451142